PHYSICAL REVIEW B VOLUME 16, NUMBER 6 15 SEPTEMBER 1977

Phonons in amorphous silica*

R. B. Laughlin and J. D. Joannopoulos
Department of Physics, Massachusetts Institute of Technology, Cambridge, Massachusetts 02139
(Received 16 May 1977)

A new theory of lattice vibrations in amorphous silicon dioxide is presented in which the randomness of the solid is treated separately from its chemistry. The theory attributes all measurable properties of phonons in silica to the nearly crystalline nearest-neighbor geometry of the lattice and to the disruptive effects of bond-angle disorder. Neutron, infrared, and Raman spectra are calculated and compared with experiment. The theory is an application of the recently developed cluster–Bethe-lattice approach to studying amorphous solids.

I. INTRODUCTION

The cluster–Bethe-lattice method[1,2] is a powerful new tool for studying the electronic and vibrational properties of amorphous solids. Its basic precept is that embedding a cluster of atoms in a solid is nearly equivalent to applying to the cluster a simple dynamic boundary condition characterizing the chemical composition of the host. It has significantly improved our understanding of amorphous solids by simplifying the mathematics used to study them theoretically.

Amorphous silicon dioxide has attracted considerable attention recently as a subject for surface studies.[3] Light scattering measurements of surface vibrations are particularly practical in silica because it is transparent, and because it is available in a porous state characterized by a very large surface-to-volume ratio. The feasibility of surface-sensitive experiments in silica has stimulated considerable interest in its surface chemistry.

As yet, no simple theory has been proposed to complement these experiments which can address the dynamic interaction between the surface and the substances adsorbed on it. Such a theory is needed to interpret and clarify the experimental results for heavy, weakly-bonded adsorbates, especially those whose vibrational bands coincide with those of the substrate. We propose to use the cluster–Bethe-lattice method to formulate a suitable theory, making use of the similarity between pores in the solid and structural defects. The cluster–Bethe-lattice method was developed for the express purpose of investigating structural defects and is ideally suited to constructing a theory of surface vibrations based on them.

In this paper, we will be concerned primarily with the preliminary aspects of the synthesis: constructing the Bethe lattice, obtaining its solution, and testing against experiment its predictions for bulk amorphous silicon dioxide. Since the behavior of surfaces is so closely tied to the behavior of the bulk, we will also concentrate in this paper on improving our *understanding* of the bulk, particularly the relative importance of the various kinds of disorder. In addition to explaining how the Bethe lattice is constructed, we wish to establish the following: (i) What in the Hamiltonian caused the features in the vibrational density of states to be where they are? (ii) How are the atoms moving? (iii) What caused the matrix elements associated with a given measurement to assume the values they do? We proceed as follows. We will first describe the Bethe lattice and explain how it functions as a boundary condition for clusters. We will then show that if it is constructed using reasonable interaction parameters, the Bethe lattice possesses a vibrational density of states similar enough to that of the actual solid to imply that *local geometry* is primarily responsible for the character of the vibrations. We will provide evidence that most of the disparity between the crystal and amorphous densities of states is due to bond-angle disorder. To establish how the atoms are moving, we will calculate local densities of states, and use them to determine how the displacements of nearby atoms correlate at low temperatures. We will then use the correlation functions to calculate neutron, infrared, and Raman spectra directly, rather than following the customary procedure of multiplying the density of states by the square of the appropriate matrix element, in order to explain from a local point of view why the spectra look as they do.

II. BETHE LATTICE

A Bethe lattice is a bonded network of atoms which has the topology of a tree. The nearest-neighbor geometry and local environment of an atom are the same as those in the actual solid, but the ordinary necessity of having rings of bonds in the structure and fluctuations in the interaction

parameters due to disorder is arbitrarily abolished. The Bethe lattice itself is a poor model for the structure of the actual amorphous solid, except in cases where lattice topology is unimportant. Its virtue lies in its exceptional simplicity and in the "transfer matrix" feature of its solution, this transfer matrix being identical to the simple boundary condition mentioned previously. The treelike topology characterizes the Bethe lattice and is responsible for its simplicity and usefulness.

We illustrate the transfer-matrix feature of the Bethe lattice with an example. Consider a tetrahedrally bonded crystal, such as germanium, which we will transform into a Bethe lattice axiomatically. We postulate that each bond may be characterized by a 3×3 matrix of spring constants D_ν which connects the atoms at either end of the bond. The index ν runs from 1 to 4 and indicates into which of the four possible directions the bond points. D_ν is a symmetric matrix.

We pick any atom and label it 0. We label its first nearest neighbors by 1 and ν_1, where ν_1 runs from 1 to 4 and indicates the direction from the central atom to the one addressed. We label the second nearest neighbors by 2, ν_1 and ν_2, where ν_1 and ν_2 now indicate the *sequence* of directions used in going from the central atom to the one in question. The third nearest neighbors are labeled by 3, ν_1, ν_2, and ν_3, and so on. In the actual solid, this labeling scheme eventually becomes redundant, as it specifies a particular path of bonds leading to the labeled atom, which cannot be unique. However, we can conveniently convert the solid into a Bethe lattice simply *by declaring every atom indexed in this manner distinct.* If this is done, the vibrational Green's function of the new treelike lattice satisfies a simple, repeating set of equations.

If we let G_{00} denote the part of the Green's function connecting atom 0 to itself, $G_{01}^{\nu_1}$ the part connecting to a first nearest neighbor, and so on, then we have

$$(\omega^2 - A)G_{00} = \sum_{\nu_1} D_{\nu_1} G_{01}^{\nu_1} + 1, \tag{1}$$

$$(\omega^2 - A)G_{01}^{\nu_1} = D_{\nu_1} G_{00} + \sum_{\nu_2 \neq \nu_1} D_{\nu_2} G_{02}^{\nu_1,\nu_2}, \tag{2}$$

$$(\omega^2 - A)G_{02}^{\nu_1,\nu_2} = D_{\nu_2} G_{01}^{\nu_1} + \sum_{\nu_3 \neq \nu_2} D_{\nu_3} G_{03}^{\nu_1,\nu_2,\nu_3}, \tag{3}$$

$$\vdots \qquad\qquad \vdots,$$

where A is the matrix of spring constants connecting an atom with itself, given from translational invariance of the Hamiltonian by

$$A = -\sum_\nu D_\nu. \tag{4}$$

We have set the masses of the atoms to 1. These equations have a solution of the form

$$G_{01}^{\nu_1} = \Phi_{\nu_1} G_{00}, \tag{5}$$

$$G_{02}^{\nu_1,\nu_2} = \Phi_{\nu_2} G_{01}^{\nu_1}, \tag{6}$$

$$\vdots,$$

provided that the four *transfer matrices* Φ_ν satisfy

$$(\omega^2 - A)\Phi_\nu = D_\nu + \sum_{\mu \neq \nu} D_\mu \Phi_\mu \Phi_\nu. \tag{7}$$

Finding the transfer matrices is a difficult task, but once they are found, the Green's function is relatively easy to construct. For example, from Eq. (1) we obtain the diagonal term

$$G_{00} = \left(\omega^2 - A - \sum_\mu D_\mu \Phi_\mu\right)^{-1} \tag{8}$$

from which the remainder of the Green's function may be constructed by repeatedly applying the transfer matrices.

Knowledge of vibrational Green's function of any large mechanical system greatly simplifies determining the vibrational behavior of molecules when they are bonded to the system. The Green's function connecting the ith atom to the jth may be thought of as the response of the ith atom to an harmonic force applied to the jth. Suppose an extra atom is bonded to the jth atom with a spring having a force constant k. If we denote the displacement of this atom by x_0 and that of the jth atom by x_j, then we have

$$M\ddot{x}_0 = F_0 = -kx_0 + kx_j, \tag{9}$$

and if the motion is harmonic, then

$$(\omega_0^2 - \omega^2)x_0 = \omega_0^2 x_j. \tag{10}$$

However, since G_{jj} describes the response of the jth atom to forces, we have

$$x_j = G_{jj} F j / M = G_{jj}\omega_0^2 (x_0 - x_j), \tag{11}$$

so that ω must satisfy the equation

$$\left(\omega^2 - \frac{\omega_0^2}{1 + \omega_0^2 G_{jj}}\right) x_0 = 0. \tag{12}$$

If we want to calculate the Green's function of the new system, the analysis proceeds along the same lines and leads to

$$G_{00} = \left(\omega^2 - \frac{\omega_0^2}{1 + \omega_0^2 G_{jj}}\right)^{-1}. \tag{13}$$

The "molecule" in this example has vibrations which are shifted and broadened with respect to the natural vibration at $\omega = 0$ because the lattice

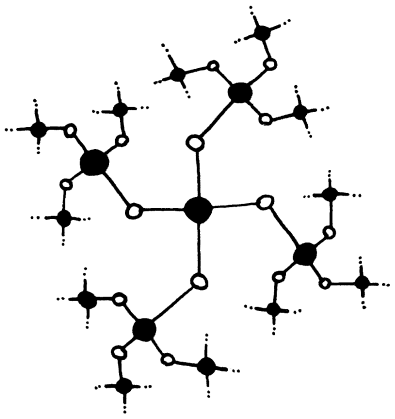

FIG. 1. Topology of the Bethe lattice. Every pair of atoms is connected by one and only one path of bonds.

"loads" the harmonic oscillator as though it were a transmission line. The diagonal Green's-function matrix element G_{jj} corresponds to the impedance of the line.

The loading of the molecule by the solid becomes more complicated when the molecule bonds to the solid in more than one place. If the molecule is connected to both atoms j and j', then the off-diagonal Green's-function matrix elements $G_{jj'}$ must be taken into account, and this necessitates inverting a matrix of rank 2. In general, if the molecule is bonded at n sites, the rank of the matrix is n. In the cluster–Bethe-lattice method, the off-diagonal matrix elements are assumed to be zero, so that each connection can be loaded independently of the others, and the Bethe-lattice Green's function, which is much simpler to calculate than that of the actual solid, is assumed to model the impedance of the solid adequately. The validity of these approximations has been verified by numerous theoretical investigations of electronic and vibrational states in amorphous solids.[1]

The silicon dioxide Bethe lattice we have constructed differs from the elementary one just described only in that it is made up of two different kinds of atoms. Its topology is illustrated in Fig. 1. Its solution is conceptually the same as that of the monatomic Bethe lattice, and its details are addressed in the Appendix.

We have used a Born-model[4] Hamiltonian in our calculation because it was used previously with great success by Bell and Dean[5] in their random-network calculation for silicon dioxide. The Born Hamiltonian assigns to each bond a potential energy of the form

$$U = \tfrac{1}{2}\alpha\left|\vec{x}-\vec{y}\right|^2+\tfrac{1}{2}(\beta-\alpha)\left|(\vec{x}-\vec{y})\cdot\hat{r}\right|^2, \tag{14}$$

where $\vec{x}$ and $\vec{y}$ are the displacements of the atoms at either end of the bond, and $\hat{r}$ is a unit vector pointing along the bond. α and β are, respectively, 4×10^5 dyn/cm and 0.7×10^5 dyn/cm. We have also employed bond angles and bond lengths approximately the same as those found in quartz. The practice of incorporating crystal parameters into Bethe lattices is well established,[1] the philosophy being that the amorphous solid is very similar to the crystal over short distances.

III. PROPERTIES OF THE SiO_2 BETHE LATTICE: DENSITIES OF STATES

We generate the density of states of the Bethe lattice from the transfer matrices using the relation[1]

$$\rho(\omega) = -\sum_j \frac{2\omega}{\pi}\mathrm{Im}[G_{jj}(\omega)], \tag{15}$$

where G_{jj} is the diagonal Green's-function matrix element associated with the jth degree of freedom. Each term in the sum is referred to as a "local density of states" because it represents the actual density of states weighted according to how much the particular degree of freedom participates in the state. We rely heavily upon local-state calculations because they give us an excellent feel for the nature of the atomic motions while being relatively easy to perform.

In our silicon dioxide Bethe lattice, atoms of a given species are all equivalent, so that there exist only six independent elementary degrees of freedom. Of these, the three associated with the oxygen atoms are particularly important because they are customarily used to identify the major features in the infrared absorption spectrum. In their early work on silicon dioxide, Bell and Dean[5] suggested that the three primary features in the density of states could be characterized as bond rocking, bond bending, or bond stretching, according to whether the oxygen atoms were moving primarily so as not to compress bonds, so as to bisect the Si-O-Si angle, or to be parallel to a line joining the two silicon neighbors, respectively. Their classification, though reasonable, has never been supported quantitatively, and for this reason we are particularly interested in the bond-rocking, bond-bending, and bond-stretching local densities of states.

In Fig. 2, we show the calculated local densities of states, comparing the three characteristic oxygen local densities of states with that of a silicon atom and with the total density of states. The three features at 450, 800, and 1080 cm^{-1} are each enhanced in the appropriate oxygen spectrum, except for the bending peak, which is accompanied by spurious features in the "bending" spectrum.

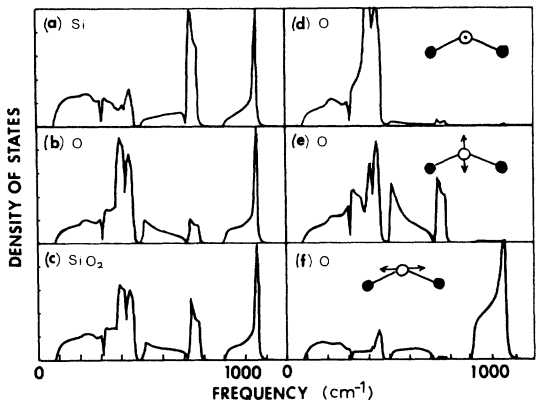

FIG. 2. Local densities of states in the silicon-dioxide Bethe lattice. (a) Average of local densities of states associated with the three degrees of freedom on a silicon atom. (b) Average of local densities of states associated with the three degrees of freedom on an oxygen atom. (c) Average density of states. (d) "Bond-rocking" local density of states. (e) "Bond-bending" local density of states. (f) "Bond-stretching" local density of states.

The peak at 800 cm^{-1} was found by Bell and Dean[5] to correspond to a complex vibration involving substantial silicon motion in addition to "bending" oxygen motion, a behavior reflected in the Bethe-lattice results. This feature is accompanied by a smaller triangle-shaped band peaking at 550 cm^{-1} which is also predominantly "bending" in character, but which does *not* involve substantial silicon motion. It is important that this latter band is the only one which is exclusively bond bending in character.

The bond-bending local density of states also manifests large features in the "rocking" bands at 450 cm^{-1}. This is most easily understood from the standpoint that "rocking" and "bending" are distinguished from one another only by the presence of the Si-O-Si bend, which in silicon dioxide has an angle of about 140°. The bend is a perturbation to the 180° Bethe lattice previously solved by Thorpe,[6] in which rocking and bending are degenerate. The bend causes part of the rocking bands to split off and become the 550-cm^{-1} feature, while it mixes the 800-cm^{-1} silicon-silicon motion with bending oxygen motion, causing this feature to show up in the bending spectrum. At 180° this feature has no oxygen character. The rocking features in the bending spectrum are the states left behind when the 500-cm^{-1} bands split off.

In Fig. 3 we compare the Bethe-lattice density of states with experiment. The neutron data shown in the figure, those of Leadbetter and Stringfellow,[7] represent the density of states of amorphous silicon dioxide modulated by a weakly varying matrix element. In order to obtain good agreement with experiment, we have artificially broadened the Bethe-lattice density of states by convolving it with a Gaussian of width 75 cm^{-1}. The amount of broadening is consistent with the disorder effects, which we will address momentarily. For completeness we have also included in Fig. 3 the density of states calculated by Bell and Dean[5] for their random network. The agreement of the Bethe-lattice density of states with experiment is tolerably good, except for the feature at 1233 cm^{-1} in the experiment. There are three oxygen features with proper widths and intensities, and a low-frequency shoulder coinciding with the acoustic-like bands of the Bethe lattice. Galeener and Lucovsky[8] have pointed out that the 1233-cm^{-1} feature results from a Lyddane-Sachs-Teller splitting of the band at 1080 cm^{-1} which, since it is due to long-range Coulomb interactions, we expect to be absent in our calculations.

In addition to Bell and Dean's classification

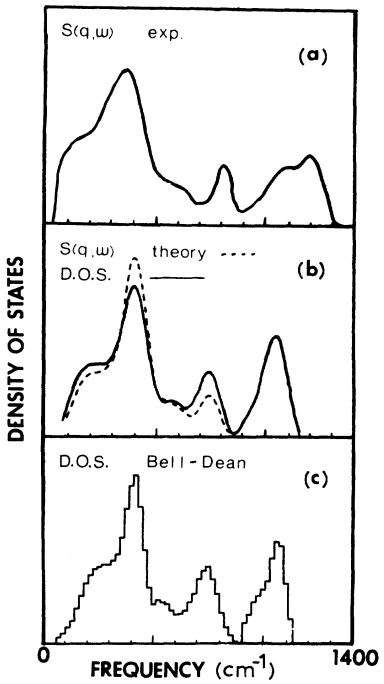

FIG. 3. Comparison of calculated density of states with neutron measurement. (a) Neutron data of Leadbetter and Stringfellow, showing density of states of silica modulated by a fairly uniform matrix element. (b) Solid curve is the calculated average density of states of silicon-dioxide Bethe lattice broadened by 75 cm^{-1}. Dotted curve is the density of states of silicon dioxide weighted as discussed in the text for comparison with neutron data. (c) Theoretical density of states for silica from random-network model of Bell and Dean.

scheme, there exists a scheme recently proposed by Galeener and Lucovsky[8] in which the vibrational bands in amorphous silicon dioxide can be viewed as dispersively broadened vibrational modes of SiO_4 molecules. Since the normal modes of an SiO_4 tetrahedron are as acceptable degrees of freedom for the Bethe lattice as the atomic displacements, we can investigate the SiO_4 nature of the vibrations by calculating the local densities of states associated with the four fundamental vibrations of a SiO_4 molecule.[9] In Fig. 4 we show the results of such a calculation, in which we use theoretical normal modes deriving from the same Born Hamiltonian used in constructing the Bethe lattice. The SiO_4 local densities of states do *not* emphasize the major features in the density of states. The projection onto the high-frequency mode diminishes the rocking bands, but leaves the high-frequency part of the density of states intact. The symmetric-stretch mode is similarly insensitive to rocking, but it is insensitive to silicon motion as well, causing the 800-cm^{-1} peak to disappear and the 1080-cm^{-1} peak to undergo distortion. The two low-frequency modes select out the rocking motions, but are distinct from one another only in which half of the peak 450 cm^{-1} they suppress. It

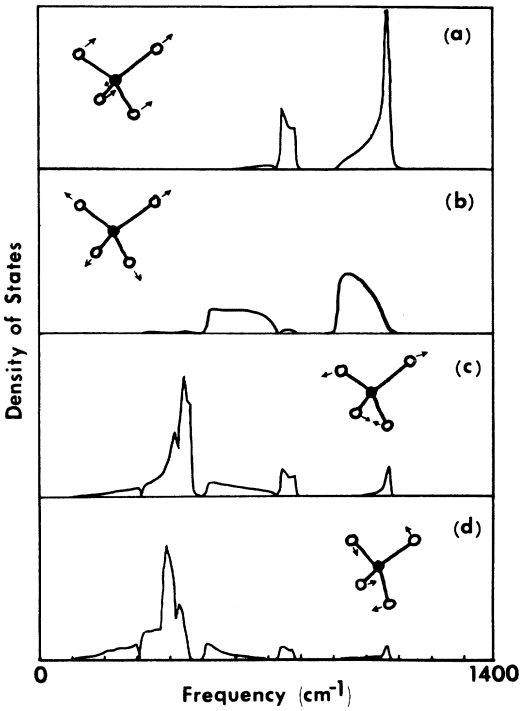

FIG. 4. Bethe-lattice density of states projected onto normal modes of SiO_4 molecule. The modes are identified in Ref. 9 in order (a)–(d) as $\nu_3, \nu_1, \nu_4, \nu_2$. Averages were performed over the degenerate modes.

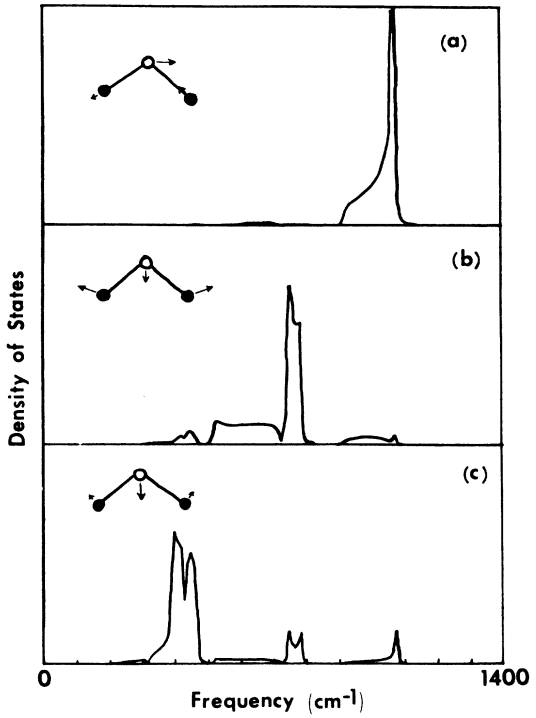

FIG. 5. Bethe-lattice density of states projected onto normal modes of Si_2O molecule. The modes are identified in Ref. 9 in order (a)–(c) as ν_3, ν_2, ν_1.

is clear that the vibrations of the Bethe lattice are not well characterized as SiO_4 normal modes.

A "molecular" model more in keeping with Bell and Dean's[5] already successful classification scheme is that of triatomic Si_2O units. Triatomic bent molecules such as H_2O have three fundamental vibrations which correspond crudely to rocking, bending, and stretching oxygen motions. The local densities of states of the Bethe lattice corresponding to these modes of an Si_2O molecule are shown in Fig. 5. The projections are much more systematic for these molecules than for SiO_4 units. Each local density of states properly emphasizes one of the three major features in the density of states, and the agreement is good enough to indicate that silica may possibly be thought of as an array of weakly interacting Si_2O molecules.

IV. DISORDER

In the bonded amorphous solid, such as silicon dioxide, we expect to find two kinds of structural disorder: topological and angular. Bond-length variations are forbidden because the distortion energies are too large, whereas bond-angle and connectivity variations are expected and observed

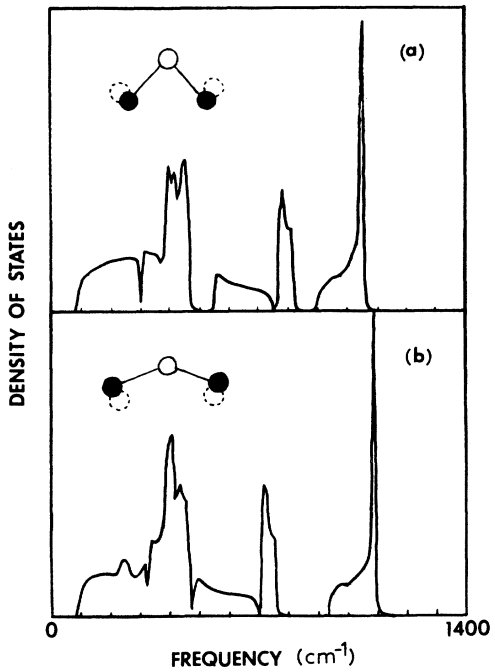

FIG. 6. Density of states of silicon dioxide Bethe lattice with every Si-O-Si angle (a) closed or (b) opened by 10° with respect to the nominal value of 138°.

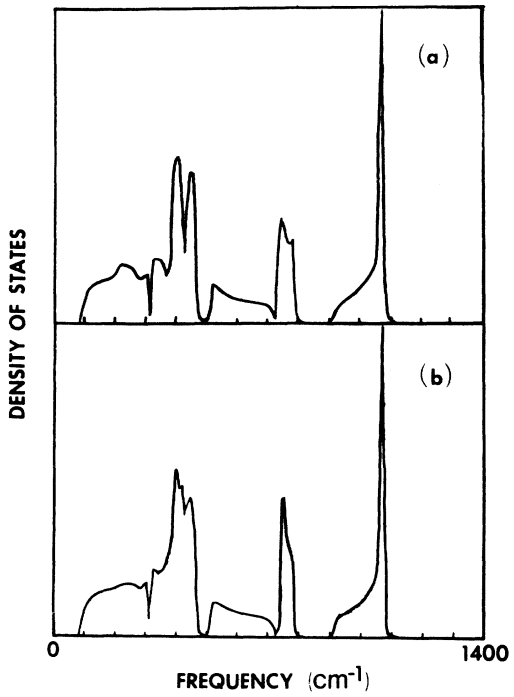

FIG. 7. Density of states of silicon dioxide Bethe lattice with every dihedral angle (a) closed or (b) opened by 10° with respect to the nominal value of 22°.

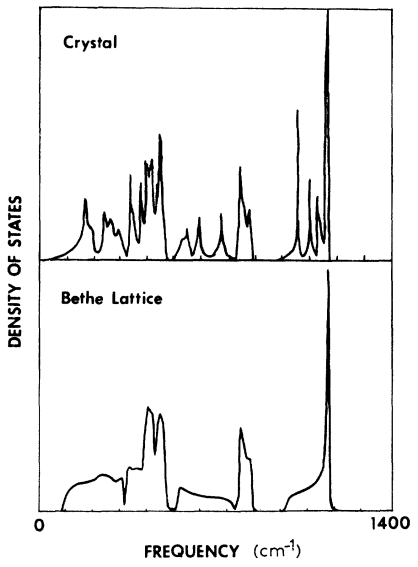

FIG. 8. Comparison of Bethe-lattice density of states with that of quartz calculated using the same Hamiltonian.

experimentally in x-ray data.[10] Si-O-Si bond-angle fluctuations of about 10° are typical for amorphous silicon dioxide,[10] and are particularly important because the positions of the features in the spectrum, especially the silicon-silicon and bond-stretching peaks, are very sensitive to this angle. In Fig. 6 we show the effect on the Bethe-lattice density of states of increasing or decreasing every Si-O-Si angle by 10°. The most important change induced in the spectrum by this distortion is lateral dispersion of the silicon-silicon and bond-stretching peaks by about 75 cm^{-1}. This displacement of the states by bond-angle fluctuations should cause a smearing of the density of states in the actual amorphous solid, and was our basis for broadening the Bethe-lattice density of states by 75 cm^{-1} when comparing it with experiment in Fig. 3. The sensitivity of the density of states to very large Si-O-Si bond angle distortions has recently been investigated by Sen and Thorpe.[11] In Fig. 7 we show the effect on the Bethe-lattice density of states of increasing or decreasing the dihedral angles by 10°. Dihedral angles have smaller distortion energies than the Si-O-Si angle and are consequently more likely to fluctuate in the amorphous solid, but the density of states is relatively insensitive to these fluctuations, so that the most important angle disorder still resides in the Si-O-Si angles.

In Fig. 8 we compare the Bethe-lattice density of states with that of quartz calculated using the same Hamiltonian. Most of the disparity between the two spectra is attributable to the predominance

of 12-fold rings of bonds in the structure of quartz. Since the types of rings of bonds most likely to form in the amorphous solid are those which form in the crystal, we expect topology to introduce features in regions where large disparities occur, such as that between 100 and 400 cm^{-1}. However, we expect the features to be less distinct than those induced by the crystal topology, as it is known[1] that the effect of topological *disorder* is generally to make the density of states more closely resemble that of the Bethe lattice.

The most important aspect of the peaks induced by the crystal topology is that they are sharp and narrow, so that when the spectrum is broadened to account for bond-angle disorder, they disappear completely, causing the spectrum to be indistinguishable from the broadened Bethe-lattice density of states. As can be seen from Fig. 3, however, the broadened Bethe-lattice density of states is itself virtually indistinguishable from that of the random network of Bell and Dean,[5] so we have established the important principle that *bond-angle disorder destroys any explicit manifestations of the network topology in the density of states of amorphous silica.* This might alternatively be viewed as a consequence of the absence of small rings of bonds in the solid.

V. INFRARED AND RAMAN SPECTRA

The other two phonon-sensitive experiments for which data on amorphous silicon dioxide are readily available are infrared absorption and Raman scattering. Neither of these is a particularly good measure of the density of states. We will test theory against these experiments by calculating theoretical spectra using the mechanisms for these processes presumed to be valid for quartz.

The usual procedure for obtaining the normal modes of the lattice and evaluating the matrix elements directly is impractical in the Bethe lattice because the normal modes are highly degenerate and difficult to orthogonalize. We surmount this problem by calculating spectra directly from the Green's function, using a simple relation between the Green's function and the displacement-displacement correlation function.

The Green's function is a sum over the normal modes of the form

$$G_{ij}(\omega)=\sum_n \frac{\vec{x}_i^{(n)}\vec{x}_j^{(n)}}{\omega^2-\omega_n^2}, \tag{16}$$

where $\vec{x}_i^{(n)}$ is the displacement of the ith atom when the lattice oscillates in its nth normal mode. ω_n is the frequency of this mode. G_{ij} is again a 3×3 matrix which operates on a force at j to produce a displacement at i:

$$\vec{x}_i=G_{ij}\cdot\vec{F}_j=\sum_n \vec{x}_i^{(n)}\left(\frac{\vec{x}_j^{(n)}\cdot\vec{F}_j}{\omega^2-\omega_n^2}\right). \tag{17}$$

Since any displacement can be expanded in terms of the normal modes

$$\vec{x}_i=\sum_n a_n\vec{x}_i^{(n)}, \tag{18}$$

we have

$$\langle\vec{x}_i\vec{x}_j^{\,*}\rangle=\sum_{n,m}\langle a_n a_m^*\rangle\vec{x}_i^{(n)}\vec{x}_j^{(m)}$$

$$=\sum_n\langle|a_n|^2\rangle\vec{x}_i^{(n)}\vec{x}_j^{(n)}, \tag{19}$$

therefore

$$\frac{1}{2\pi}\int\langle\vec{x}_i(0)\vec{x}_j^{\,*}(t)\rangle e^{i\omega t}dt$$

$$=\sum_n\left(\frac{1}{2\pi}\int\langle a_n(0)a_n^*(t)\rangle e^{i\omega t}\,dt\right)\vec{x}_i^{(n)}\vec{x}_j^{(n)}$$

$$=\sum_n f(\omega)\delta(\omega-\omega_n)\vec{x}_i^{(n)}\vec{x}_j^{(n)}, \tag{20}$$

where $f(\omega)$ is a function of frequency which depends on the temperature. However, the imaginary part of the Green's function also takes this form

$$\mathrm{Im}[G_{ij}(\omega)]=-\frac{\pi}{2\omega}\sum_n\delta(\omega-\omega_n)\vec{x}_i^{(n)}\vec{x}_j^{(n)}, \tag{21}$$

so we have

$$\frac{1}{2\pi}\int\langle\vec{x}_i(0)\vec{x}_j^{\,*}(t)\rangle e^{i\omega t}dt$$

$$=-\frac{2\omega f(\omega)}{\pi}\,\mathrm{Im}[G_{ij}(\omega)]. \tag{22}$$

Referring back to Fig. 2, we see that the *diagonal* correlations of the Bethe lattice are already quite different from one another, these differences being associated with the slight enhancement of the 450-cm^{-1} peak in the neutron spectrum of Fig. 3 over the theoretical value. Inelastic neutron scattering measures the dynamical structure factor $S(\vec{q},\omega)$,[12] which is related to the correlation function by

$$S(\vec{q},\omega)\propto\sum_{i,j}\left(\frac{1}{2\pi}\int\langle\vec{q}\cdot\vec{x}_i(0)\vec{x}_j(t)\cdot\vec{q}\rangle e^{i\omega t}dt\right)$$

$$\times e^{i\vec{q}\cdot(\vec{R}_i-\vec{R}_j)}, \tag{23}$$

where $\vec{R}_i$ is the position vector of the ith atom. This may also be written in terms of the Green's function.

$$S(\vec{q},\omega)\propto-\mathrm{Im}\left(\sum_{i,j}\vec{q}\cdot G_{ij}\cdot\vec{q}\,e^{i\vec{q}\cdot(\vec{R}_i-\vec{R}_j)}\right). \tag{24}$$

The particular experiment we refer to evaluates

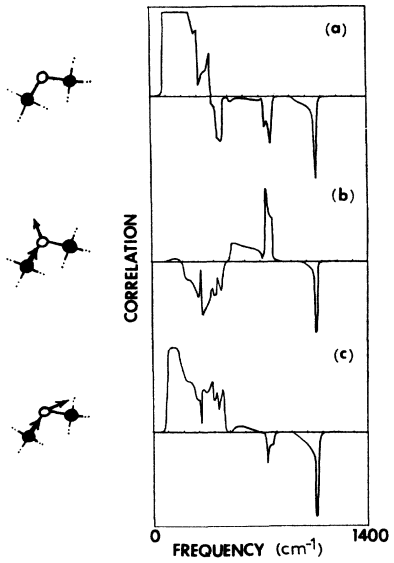

FIG. 9. Nearest-neighbor correlation functions in the Bethe lattice. (a) Trace of the correlation matrix, showing negative correlation in the infrared-active bands. (b) Silicon motion along the bond correlated with "bending" oxygen motion, showing tendency at 800 cm^{-1} for silicon atoms to squeeze oxygen atoms in the bending direction. (c) Silicon motion along the bond correlated with "stretching" oxygen motion, showing tendency of atoms to move together in the acoustic-like bands.

$S(\vec{q}, \omega)$ at high-momentum transfers $\vec{q}$, in the so-called "incoherent limit," where configurational fluctuations in nearest-neighbor distance cause the off-diagonal correlations to contribute nothing to the scattering cross section. Since the local densities of states derive from the *reduced* Green's function, they are converted to mean-square displacements by dividing by the mass of the atom. This implies that the oxygen local densities of states are weighted more in the neutron spectrum than they are in the total density of states. The difference in the neutron cross sections for the different nuclei enters in as well, the net result being to overemphasize the oxygen local density of states by about a factor of 2. The dotted curve in Fig. 3 is a theoretical neutron spectrum.

While the off-diagonal correlations do not contribute to the neutron spectrum, they are extremely important in the other two experiments. For example, in Fig. 9(a) the trace of the nearest-neighbor correlation matrix reveals strong negative correlations between silicon and oxygen displacements at 450, 800, and 1080 cm^{-1}, which causes the infrared activity of these bands. Modes of heteropolar solids are infrared active when dissimilar atoms vibrate out of phase. The strong positive correlation at 200 cm^{-1} is associated with the acoustic-like bands of the Bethe lattice and suppresses their infrared activity. In Fig. 10(c) we see very strong "bending-bending" correlation at 500 cm^{-1} associated with a very intense Raman band. The proposed mechanism for Raman scattering[13] in quartz is the dilation of the electronic polarizability by the oxygen atoms when they move in the "bending" direction.

The infrared experiment measures the phonon contribution to the dielectric function in a solid. We evaluate this theoretically by means of the formula

$$\epsilon = 1 + \frac{4\pi}{v} \sum_{i,j} Q_i G_{ij} Q_j + 4\pi \chi_{\text{electrons}}, \tag{25}$$

where v is the volume of the solid and Q_i is the charge on the ith atom. Rather than viewing G as a correlation function in this expression, it is convenient to think of it as describing the dipole moment induced on atom i resulting from applying a force $Q_j \vec{E}$ to atom j.

In Fig. 11 we compare with experiment the imaginary part of the phonon contribution in (25) summed *not* over the entire solid, but over a 33-atom nucleus in the Bethe lattice. The Bethe lattice is

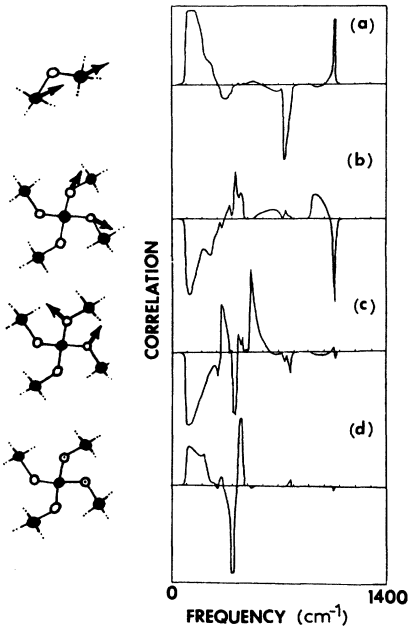

FIG. 10. Second-nearest neighbor correlation functions in the Bethe lattice. (a) Silicon-silicon correlation showing squeezing effect at 800 cm^{-1}. (b) Stretching-stretching correlation. (c) Bending-bending correlation showing strong positive value at 550 cm^{-1} associated with Raman activity. (d) Rocking-rocking correlation. All oxygen-oxygen correlations are between "1" and "2" atoms as defined in the text.

topologically identical to quartz up to fifth-nearest neighbors, due to the absence of small rings of bonds in quartz. If we assume that the same holds true for the amorphous solid, we can approximate the actual Green's function with the Bethe-lattice Green's function for fifth-nearest neighbors and closer. The 33-atom cluster just includes fifth-nearest neighbors of the central atom. Restricting the sum (25) to such a cluster in the actual solid would lead to large errors; however, the *trends* would be right. If the cluster were diminished to one atom, the sum would produce a local density of states. If it were extended to the whole solid, the sum would produce the correct spectrum. If we discover how the density of states is weighted when the sum is taken over an intermediate system, we can infer how it will be weighted when the sum is done correctly. In the calculation we use the effective charge tensors Q_i found by Kleinman and Spitzer to be appropriate for quartz.[13] The theory has been artificially broadened by 75 cm^{-1}. The experimental spectrum is that of Galeener and Lucovsky.[8] The agreement between theory and experiment is excellent, except for the excessive width of the peak at 450 cm^{-1}, which we believe to be due to the small size of the cluster over which the sum was taken. We conclude that the Bethe lattice is consistent with the infrared data.

Agreement of the Bethe lattice with existing Raman data is less good. The mechanism used with moderate success by Kleinman and Spitzer[13] to account for the intensities of the four A_1 Raman lines in quartz involves an isotropic dialation of a scalar polarizability by the atoms when they move so as to compress bonds. Kleinman and Spitzer observed that the Raman intensities were harder to fit than the infrared intensities. They did not address the eight E lines in the Raman spectrum.

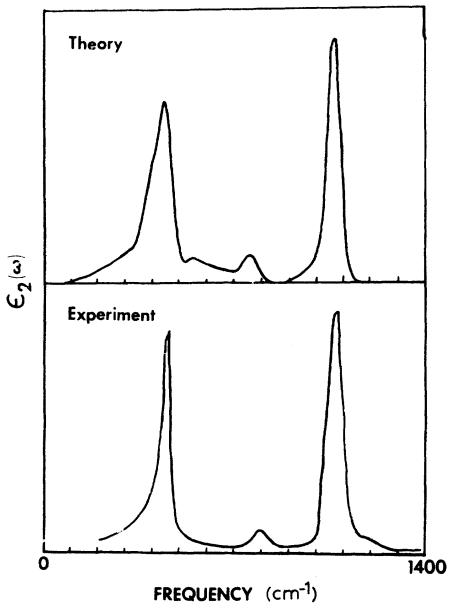

FIG. 11. Theoretical vs experimental values for the phonon contribution to $\epsilon_2(\omega)$ in silica.

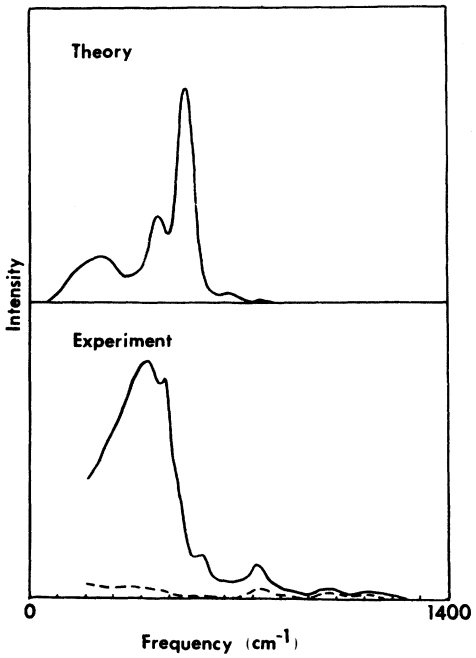

FIG. 12. Theoretical vs experimental values for the reduced Raman spectrum of silica. The dotted curve is the H-V spectrum, which is identically zero in the theory. The solid curve is the V-V spectrum.

The Raman cross section is given by[14]

$$\frac{d\sigma}{d\Omega} \propto \sum_{i,j} \left(\int \langle \delta\alpha_i(0)\delta\alpha_j(t)\rangle e^{i\omega t}\, dt \right) e^{i\vec{q}\cdot(\vec{R}_i - \vec{R}_j)}, \qquad (26)$$

where $\delta\alpha_i$ is the change in the electronic polarizability at atom i. If we let $\vec{\nabla}\alpha_i$ denote the gradient of α_i with respect to $\vec{x}_i$, we obtain for the small-momentum transfers $\vec{q}$ of light scattering

$$\frac{d\sigma}{d\Omega} \propto \sum_{i,j} (\vec{\nabla}\alpha_i) \cdot \left(\int \langle \vec{x}_i(0)\vec{x}_j(t)\rangle e^{i\omega t}\, dt \right) \cdot (\vec{\nabla}\alpha_j)$$

$$= -\frac{2\omega f(\omega)}{\pi} \sum_{i,j} (\vec{\nabla}\alpha_i) \cdot \mathrm{Im}[G_{ij}(\omega)] \cdot (\vec{\nabla}\alpha_j). \qquad (27)$$

We approximate this expression as before by summing over a 33-atom cluster in the Bethe lattice.

In Fig. 12 we compare our results with the experimental spectrum of Galeener and Lucovsky.[8] The theory has again been artificially broadened

by 75 cm^{-1}. The intense peak at 550 cm^{-1} in the theory is probably the feature at 500 cm^{-1} in the experiment. It is too strong and in the wrong place in the theory. The band between 100 and 400 cm^{-1} is shifted upward and is too weak in the theory. We can rectify this problem by adopting the more sophisticated Keating[15] Hamiltonian—however, the 500-cm^{-1} peak seems to be a property of bond-oriented Hamiltonians. The rest of the features in the experimental spectrum, except for the one at 600 cm^{-1}, may be reproduced by adopting an additional small *depolarizing* mechanism for the Raman effect. It has been suggested[8] that this feature at 600 cm^{-1} is a defect state. We have not yet been able to identify it as such. We conclude from the Raman calculation that the Bethe lattice is somewhat inaccurate in the region of 200 cm^{-1} and very inaccurate at 550 cm^{-1} because it is constructed using nearest-neighbor interactions only.

VI. SUMMARY AND CONCLUSIONS

The Bethe lattice provides a simple means of investigating explicitly the effects of local geometry, topology, and disorder on the vibrational spectrum of an amorphous solid. Using Born-model interactions and the configurations of nearest neighbors found in quartz, we have constructed a Bethe lattice for silicon dioxide and have used it both to analyze neutron, infrared, and Raman experiments, and to investigate the effects of disorder. Several new facts about amorphous silica have emerged from this study: (i) The vibrational properties of amorphous silica are completely dominated by local effects, particularly the values of the bond angles in the immediate vicinity of an atom. (ii) Bond-angle fluctuations are important only in that they broaden features in the spectra that would otherwise be sharp. (iii) The topology of amorphous silica is not manifested in any available data. (iv) Phonons in amorphous silica are not characteristically SiO_4-like. (v) Matrix-element effects in neutron, infrared, and Raman experiments are *local* phenomena.

ACKNOWLEDGMENTS

We are grateful to the Alfred P. Sloan Foundation and IBM for financial support.

APPENDIX: THE SILICON DIOXIDE BETHE LATTICE

We first set up local coordinates on each silicon atom and make them identical by requiring that the coordinates of the nearest-neighbor oxygen atoms always be the same. The oxygen neighbors are positioned at the vertices of a perfect tetrahedron and numbered 1 through 4. For convenience, we introduce a 3×3 matrix S which rearranges the bonds according to a cyclic permutation σ. Letting D_ν denote the dynamical matrix connecting the central silicon atom and the νth oxygen atom, we have

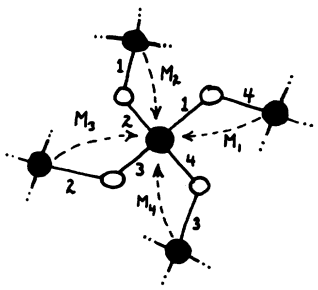

FIG. 13. Bond-matching rules for silicon dioxide Bethe lattice.

$$SD_\nu S^{-1} = D_{\sigma(\nu)}. \tag{A1}$$

We also introduce four orthogonal matrices M_ν which transform vectors from the four neighbor silicon coordinate systems into the central silicon coordinate system, and which contain the bond-angle information. These are taken to be symmetries of crystalline silicon dioxide, and have the following properties:

$$\text{(a)}\quad M_\nu = S^2 M_{\sigma(\nu)}^{-1}, \tag{A2}$$

$$\text{(b)}\quad M_1^3 = 1, \tag{A3}$$

$$\text{(c)}\quad M_1 = M_2 S^2. \tag{A4}$$

There are two symmetries of the crystal which transform a silicon atom to its neighbor. The first rule expresses the arbitrary selection of the one of these which attaches a ν bond and a $\tau(\nu)$ bond to the same oxygen atom. There is no symmetry which attaches the same bond to both sides. The bond matching convention is illustrated in Fig. 13. The second rule expresses the threefold rotational symmetry of the crystal. The third expresses the translational symmetry connecting atoms 1 and 2. These axioms are sufficient to generate the four transformations, and lead to a Si-O-Si angle given by

$$\cos\theta = -\tfrac{1}{3}\sqrt{5} \tag{A5}$$

and a dihedral angle given by

$$\cos\psi = (3+\sqrt{5})/4\sqrt{2}. \tag{A6}$$

The dynamical matrix connecting the silicon atom with itself is constrained by translational invariance of the total Hamiltonian to be

$$A = -\sum_\nu D_\nu, \tag{A7}$$

and the matrix B_ν connecting the νth oxygen atom with itself is similarly given by

$$B_\nu = -(D_\nu + M_\nu D_{\sigma(\nu)} M_\nu^{-1}). \tag{A8}$$

Using these dynamical matrices appropriately reduced by the silicon and oxygen masses we generate a repeating sequence of equations describing the vibrational Green's function in the frequency domain. If we let G_0 denote the 3×3 submatrix of the Green's function connecting a silicon atom with itself, $F_1^{\nu_1}$ the submatrix connecting the silicon atom with the ν_1th oxygen neighbor, $G_1^{\nu_1}$ the submatrix connecting to the ν_1th silicon neighbor, and so on, then we have

$$(\omega^2 - A)G_0 = 1 + \sum_{\nu_1} D_{\nu_1} F_1^{\nu_1}, \tag{A9}$$

$$(\omega^2 - B_{\nu_1})F_1^{\nu_1} = D_{\nu_1} G_0 + M_{\nu_1} D_{\sigma(\nu_1)} G_1^{\nu_1}, \tag{A10}$$

$$(\omega^2 - A)G_1^{\nu_1} = D_{\sigma(\nu_1)} M_{\nu_1}^{-1} F_1^{\nu_1} + \sum_{\nu_2 \neq \sigma(\nu_1)} D_{\nu_2} F_2^{\nu_1,\nu_2}, \tag{A11}$$

$$(\omega^2 - B_{\nu_2})F_2^{\nu_1,\nu_2} = D_{\nu_2} G_1^{\nu_1} + M_{\nu_2} D_{\sigma(\nu_2)} G_2^{\nu_1,\nu_2}, \tag{A12}$$

$$\vdots \qquad\qquad \vdots$$

$$(\omega^2 - A)G_n^{\nu_1,\cdots,\nu_n} = D_{\sigma(\nu_n)} M_{\nu_n}^{-1} F_n^{\nu_1,\cdots,\nu_n} + \sum_{\nu_{n+1}\neq\sigma(\nu_n)} D_{\nu_{n+1}} F_{n+1}^{\nu_1,\cdots,\nu_{n+1}}. \tag{A13}$$

$$(\omega^2 - B_{\nu_n})F_n^{\nu_1,\cdots,\nu_n} = D_{\nu_n} G_{n-1}^{\nu_1,\cdots,\nu_{n-1}} + M_{\nu_n} D_{\sigma(\nu_n)} G_n^{\nu_1,\cdots,\nu_{n+1}}. \tag{A14}$$

To solve this system we first eliminate every other equation to obtain

$$\tilde{A} G_n^{\nu_1,\cdots,\nu_n} = \tilde{D}_{\nu_n}^t G_{n-1}^{\nu_1,\cdots,\nu_{n-1}} + \sum_{\nu_{n+1}\neq\sigma(\nu_n)} \tilde{D}_{\nu_{n+1}} G_{n+1}^{\nu_1,\cdots,\nu_{n+1}}, \tag{A15}$$

where

$$\tilde{A} = \omega^2 - A - \sum_\nu D_\nu (\omega^2 - B_\nu)^{-1} D_\nu \tag{A16}$$

and

$$\tilde{D}_\nu = D_\nu (\omega^2 - B_\nu)^{-1} M_\nu D_{\sigma(\nu)}. \tag{A17}$$

A solution of the form

$$G_{n+1}^{\nu_1,\cdots,\nu_{n+1}} = \Phi_{\nu_{n+1}} G_n^{\nu_1,\cdots,\nu_n} \tag{A18}$$

is then substituted, which leads to recursion relations for the transfer matrices Φ_ν of the form

$$\Phi_\nu = \left(\tilde{A} - \sum_{\mu\neq\sigma(\nu)} \tilde{D}_\mu \Phi_\mu\right)^{-1} \tilde{D}_\nu^t. \tag{A19}$$

These equations are solved numerically by iterating the continued fraction starting from $\Phi_\nu = 0$. Once the transfer matrices are found, G_0 may be calculated using the relation

$$G_0 = \left(\tilde{A} - \sum_\mu \tilde{D}_\mu \Phi_\mu\right)^{-1} \tag{A20}$$

and the remainder of the Green's function constructed from G_0.

*Supported in part by the U. S. Navy ONR Grant No. N00014-77-6-0132.

[1]J. D. Joannopoulos and F. Yndurain, Phys. Rev. B 10, 5164 (1974).
[2]C. Domb, Adv. Phys. 9, 145 (1960).
[3]Edgerton and Hardin, Catal. Rev. Sci. Eng. 11, 71 (1975).
[4]M. Born, Ann. Phys. (Leipz.) 44, 605 (1914).
[5]R. J. Bell, N. F. Bird, and P. Dean, J. Phys. C 1, 299 (1968).
[6]M. F. Thorpe, AIP Conf. Proc. 31, 251 (1976).
[7]A. J. Leadbetter and M. W. Stringfellow, Neutron Inelastic Scattering, Proceedings of the Grenoble Conference (IAEA), Vienna, 1972 (unpublished), p. 501.
[8]F. Galeener and G. Lucovsky, Phys. Rev. Lett. 37, 1474 (1976).
[9]G. Hertzberg, *Infrared and Raman Spectra* (Van Nostrand, New York, 1945).
[10]P. H. Gaskell and D. W. Johnson, J. Non-Cryst. Solids, 20, 171 (1976).
[11]P. Sen and M. F. Thorpe, Phys. Rev. B 15, 4030 (1977).
[12]B. T. M. Willis, *Chemical Applications of Thermal Neutron Scattering* (Oxford U.P., London, 1973), p. 26.
[13]D. A. Kleinman and W. G. Spitzer, Phys. Rev. 125, 16 (1962).
[14]R. Shuker and R. W. Gammon, Phys. Rev. Lett. 25, 222 (1970).
[15]P. N. Keating, Phys. Rev. 145, 637 (1966).